

# RSC Advances



This is an *Accepted Manuscript*, which has been through the Royal Society of Chemistry peer review process and has been accepted for publication.

*Accepted Manuscripts* are published online shortly after acceptance, before technical editing, formatting and proof reading. Using this free service, authors can make their results available to the community, in citable form, before we publish the edited article. This *Accepted Manuscript* will be replaced by the edited, formatted and paginated article as soon as this is available.

You can find more information about *Accepted Manuscripts* in the [Information for Authors](#).

Please note that technical editing may introduce minor changes to the text and/or graphics, which may alter content. The journal's standard [Terms & Conditions](#) and the [Ethical guidelines](#) still apply. In no event shall the Royal Society of Chemistry be held responsible for any errors or omissions in this *Accepted Manuscript* or any consequences arising from the use of any information it contains.

## Enhance carrier transport in Tris(8-hydroxyquinolate) aluminum by Titanyl Phthalocyanine doping

M. Ramar, Priyanka Tyagi, C.K.Suman\*, Ritu Srivastava

CSIR-Network of Institutes for Solar Energy  
Physics of Energy Harvesting division  
CSIR-National Physical Laboratory, New Delhi, India

### Abstract:

The doping effect of Titanyl phthalocyanine (TioPc) in Tris(8-hydroxyquinolate) aluminum ( $\text{Alq}_3$ ) ( $\text{Alq}_3\text{:T}$ ; where T represents TioPc) used as electron transport layer (ETL) for organic light emitting diodes (OLEDs) was investigated. The surface roughness of the doped thin films increases with doping concentration as a result of needle like 3D growth of TioPc in  $\text{Alq}_3$ . The electron mobility depends on doping concentration. Electron mobility calculated in the trap-free space-charge limited region (SCLC) for 2% doped  $\text{Alq}_3$  thin film was found to be  $0.17 \times 10^{-5} \text{ cm}^2 \text{V}^{-1} \text{s}^{-1}$  which is of four orders in compare to pristine  $\text{Alq}_3$ . The electroluminescence at a constant current density of  $10 \text{ mA/cm}^2$  is 3098, 4700, 7800, 3600 and  $520 \text{ cd/m}^2$  for  $\text{Alq}_3$  to  $\text{Alq}_3\text{:T}$  (1%, 2%, 3% and 5%) devices, respectively. Similarly the power efficiency at constant current density of  $10 \text{ mA/cm}^2$  is 2.1, 2.7, 4.2, 1.3 and  $0.48 \text{ lm/W}$  for the different doping device  $\text{Alq}_3$  to  $\text{Alq}_3\text{:T}$  (1%, 2%, 3% and 5%), respectively. The optimized 2% doped TioPc in  $\text{Alq}_3$  based OLEDs shows four times increase in electroluminescence as well as almost double of power efficiency. There are interfacial charges near the doped layer. The Cole-Cole plot indicates the device can be modeled as the combination of three parallel resistance-capacitance ( $R\text{-C}$ ) equivalent circuits.

**Keywords:** TioPc, doped, carrier injection, trap-free, mobility.

\* Corresponding author

[cksuman@gmail.com](mailto:cksuman@gmail.com)

## Introduction

Since first successful demonstration of organic light emitting diodes (OLEDs) by Tang and Van Slyke [1,2], good steady progress has been made in improving these devices for use in practical applications. The power consumption and reliability of OLEDs have been key issues for real applications and have shown remarkable progress through intensive research in the past decade [3-5]. Functional devices based on conjugated polymers or small molecules such as light emitting diodes (OLEDs), organic solar cells (OSC) and organic field - effect transistor (OFETs) have great potential toward light weight, flexible and low-cost electronic and optoelectronic applications [6]. To obtain highly efficient and low-voltage OLEDs, optimization of charge injection and carrier transport is critically important towards the improvement of device performance. [7,8] The doping of organic semiconductors was first studied in the year 1960 [9], however they have been extensively studied only after their use in enhancing the charge carrier injection and transport properties in optoelectronic devices [10-15], such as OLEDs and OSC. Despite the extensive studies on p-type, n-type doping of organic semiconductors, Doping optimization in organic semiconductor still remains a challenge.

In all of these organic device embodiments, optimization of charge injection/extraction and carrier transport is critically important towards their technological success [16-18]. Efficient injection or extraction requires low energetic barriers while competent transport demands highly conductive transport layers. Organic semiconductors have low carrier concentration and low carrier mobility [18, 19]. A widely used method for improving electron injection and transport is to employ low-

work-function metals, either as individual layer in contact with cathode or as n-type conductive dopants in the organic electron-injection layers (EILs), which can help to reduce the injection barrier at the electrode/organic interface and provide excellent electron injection from cathode to organic layer [20-24]. Alkali metals like Li, Cs and their oxides are also used for n-type conductive doping of organic electron transport materials [25-27] and were found useful in many instances. But this type of doping has lots of problems, like damage to underlying organic layers due to the tendency to diffuse in the organic materials. Due to this reason, there is a need for molecular dopants for enhancement of electron transporting properties and its use in OLED applications.

Here, we have compared the TioPc as the n-type dopant of Alq3 with different concentrations. The thin films of doped and undoped films were studied and checked for the application of lighting devices (OLEDs)

### **Experimental methods**

The electron only devices were fabricated with the structure of Al|Alq3:TioPc|Al. The Alq3 is doped with TioPc by weight percentage doping concentration of 1,2,3 and 5%; those thin films and devices were named as Alq3, Alq3:T1, Alq3:T2, Alq3:T3 and Alq3:T5, respectively. The doping of organic layers was performed by thermal co-evaporation process. Similarly; Light emitting diode (OLEDs) was fabricated on indium-tin-oxide (ITO) (purchased from Vin Karola USA) coated glass substrates with a sheet resistance of 20  $\Omega$ /sq. Before depositing all organic materials, ITO substrates were cleaned ultrasonically with de-ionized water, acetone and isopropyl alcohol and finally dried them. The deposition rate was kept 1-2  $\text{\AA}/\text{s}$  for organic layers and 2-5  $\text{\AA}/\text{s}$

for aluminum as metal cathode. The overlap of ITO anode and Al cathode defines the active area of the device to be 6 mm<sup>2</sup>.

Current density-voltage (*J-V*), current density-voltage-luminescence (*J-V-L*) and current efficiency-current density-power efficiency characteristics of OLEDs were measured simultaneously with a programmable Keithley 2400 power source and Luminance meter (LMT-1009). Impedance spectroscopy (IS) measurement was performed by using Impedance/Gain-Phase Analyzer (Solartron, model SI 1260) Characterization System. A 100 mV amplitude AC signal superimposed on a DC bias was used to measure device impedance as a function of AC frequency and DC bias.

## Results and discussion

The surface morphologies of doped and undoped Alq<sub>3</sub> thin films were characterized by atomic force microscopy (AFM). Figure 1 (A)-(E) show the AFM images of Alq<sub>3</sub>, Alq<sub>3</sub>:T1, Alq<sub>3</sub>:T2, Alq<sub>3</sub>:T3 and Alq<sub>3</sub>:T5. The surface roughness increases with increasing concentration of TiOPc. The RMS values of roughness are 0.3914 nm, 0.5549 nm, 0.5742 nm, 0.6146 nm and 6.2326 nm for Alq<sub>3</sub>, Alq<sub>3</sub>:T1, Alq<sub>3</sub>:T2, Alq<sub>3</sub>:T3 and Alq<sub>3</sub>:T5 respectively. The thin film of Alq<sub>3</sub>, Alq<sub>3</sub>:T1 and Alq<sub>3</sub>:T2 consists of small uniform 3D islands with a compact shape. The surface morphology changes drastically if doping concentration was increased from 2%: island shape transition occurs resulting in typical needle-like structures with elongated 3D-islands. Figure 2(E) show that the islands become thereby progressively longer, quickly reaching a fixed asymptotic width while their height remains much longer than their width. Hence it is not suitable to have high doping concentration of TiOPc for device application.

Since Al work function is about 4.2 eV and the Alq<sub>3</sub> LUMO value is 3.0 eV [28], the electron injection between Al and Alq<sub>3</sub> will be very high. However, in between Al and Alq<sub>3</sub> films it is observed that there are large interface dipoles present [29], which reduces electron injection barrier by about 1.0 eV hence the net barrier present is now 0.2 eV. In the same way, the energy barrier for hole injection is increased by 1.0 eV due to interface dipole and the resultant barrier for hole injection turns to 2.5 eV. Therefore, hole is not injected in compare to electron injection, and any current observed in the device will be only due to electrons flowing between two Al electrodes. Therefore, the electron only devices can be considered in the structure of Al/organic/Al. The thicknesses of organic films were kept at 100 nm for all the five devices. Figure 2 shows the *J-V* characteristics of electron only Alq<sub>3</sub>, Alq<sub>3</sub>:T1, Alq<sub>3</sub>:T2, Alq<sub>3</sub>:T3 and Alq<sub>3</sub>:T5 devices. The inset of figure 2 shows the enlarged *J-V* characteristics taking x axis as log scale. It is clearly shown in the inset figure that the driving voltage of the electron only device shifts with doping concentration. The current density increases linearly with the increase of voltage in low region, at high region the current density increases non-linearly for all the devices. At low voltages (first region of I-V curve), the slope of the Log I-V plots are approximately unity, while at higher voltages, the slope is about 2 or more. Hence the conductivity is clearly Ohmic at low voltage and space charge limited conductivity (SCLC) at higher voltages. In the Ohmic region of the conductivity, the current density  $J = qn_0\mu\frac{v}{d}$ , Where  $n_0$  is the concentration of thermally activated carriers,  $\mu$  is the mobility and  $d$  is the thickness of the organic semiconductor used ( $d$  =100nm). At high voltages region (second region of I-V curve)  $J \propto V^2$  indicates a limited current controlled by a space charge with a single discrete set of shallow traps. The

current density in this region is  $J = \frac{9}{8} \epsilon \mu \theta \frac{V^2}{d^3}$ , Where  $\epsilon$  is the organic semiconductor dielectric constant (taken as 3.5),  $\mu$  is the charge carrier mobility and  $\theta$  is the trapping fraction. The trapping fraction can be represented by  $\theta = \frac{n_o}{n_o + n_t}$ , Where  $n_o$  is the free charge carrier density and  $n_t$  is the trapped charge carrier density. The electron mobility of Alq<sub>3</sub> calculated assuming trap free SCLC ( $n_t = 0$ ) was  $0.62 \times 10^{-8} \text{ cm}^2 \text{ V}^{-1} \text{ s}^{-1}$  which is comparable to the mobility obtained from the TOF technique [30]. The mobility for doped thin film are  $0.7 \times 10^{-7}$ ,  $0.17 \times 10^{-5}$ ,  $0.75 \times 10^{-6}$  and  $0.68 \times 10^{-9} \text{ cm}^2 \text{ V}^{-1} \text{ s}^{-1}$  for Alq<sub>3</sub>:T1, Alq<sub>3</sub>:T2, Alq<sub>3</sub>:T3 and Alq<sub>3</sub>:T5, respectively. The mobility for Alq<sub>3</sub>:T2 thin film is higher than all the four different concentration of doped thin film. The electron mobility of Alq<sub>3</sub>:T2 thin film is of four orders in compare to Alq<sub>3</sub> device. The suitable doping concentration opens the new hopping sites for the carrier that leads to increase of mobility in organic semiconductor. The other reasons for the enhancement of electron mobility may be broadening of density of states and charge transfer [31]. The common inorganic insulator (Li salts) doping in Alq<sub>3</sub> creates radical ions of Alq<sub>3</sub> responsible for the n type doping effect. Similar negative charge enriched thin films are achieved by organic molecular doping.[32]

Figure 3 show (A) the energy level diagram of the OLED (B) the electroluminescence spectra of the device at different bias voltage; inset of figure B shows the camera image of light output at bias voltage of 8V and 15V. The fabricated OLED structure consists of 35 nm N,N'-di(naphthalene-1-yl)-N,N'-diphenyl-benzidine (NPB) as hole-transporting layer (HTL), 35 nm tris(2-phenylpyridine)iridium(III) [Ir(ppy)<sub>3</sub>] (5%) doped in 4,4'-bis-(corbozol-9-yl)-biphenyl (CBP) green light emitting layer (EML), 6 nm-thick 2,9-

dimethyl-4,7-diphenyl-1,10-phenanthroline (BCP) hole-blocking layer (HBL) and 28 nm-thick Titanyl phthalocyanine (TiOPc) doped Tris(8-hydroxyquinolato) aluminum ( $\text{Alq}_3$ ) electron transport layer (ETL). The doping of  $\text{Ir}(\text{ppy})_3$  in CBP facilitated the control of triplet quenching at the interfaces. ITO and Lithium fluoride (LiF) (1 nm)/Aluminium (Al) (100 nm) were used for the anode and cathode, respectively. The device structure of green phosphorescent OLEDs is [ITO/NPB/CBP: $\text{Ir}(\text{ppy})_3$ /BCP/ $\text{Alq}_3$ :T(x)/LiF/Al]. EL spectra showed an emission only from  $\text{Ir}(\text{ppy})_3$  with no emission from neighboring materials. The emission pattern is in the green spectral range of the visible regime, with its main peaks at 515nm and an additional shoulder at 550nm. There is no significant shift in the position of the emission peaks with the applied bias range. The emission color is stable in the investigated bias voltage region.

Figure 4 shows the *J-V-L* characteristics of OLEDs containing  $\text{Alq}_3$ ,  $\text{Alq}_3$ :T1,  $\text{Alq}_3$ :T2,  $\text{Alq}_3$ :T3 and  $\text{Alq}_3$ :T5 as the ETLs, respectively. The current density at high voltage increases with TiOPc doping concentration upto 2%, above 2% doping the value of current density is found to be low in compare to undoped ETL. At fixed bias of 11 V, the current density of devices  $\text{Alq}_3$ ,  $\text{Alq}_3$ :T1,  $\text{Alq}_3$ :T2,  $\text{Alq}_3$ :T3 and  $\text{Alq}_3$ :T5 are 57.81, 24.35, 72.35, 47.62 and 11.26  $\text{mA}/\text{cm}^2$ , respectively. The current density of  $\text{Alq}_3$ :T2 OLED increased 25 % compare to pristine  $\text{Alq}_3$  device. The driving voltage is reduced for T2 device that indicates the enhancement of electron injection and transport by suitable ETLs. The luminescences at a current density 10  $\text{mA}/\text{cm}^2$  of devices  $\text{Alq}_3$  to  $\text{Alq}_3$ :T5 are 3098, 4700, 7800, 3600 and  $\text{cd}/\text{m}^2$ , respectively. At this value of current density, the increase in luminescence is two times. This enhancement in electroluminescent may be attributed to the enhancement of holes and electrons recombination rate.

Figure 5 (a) and (b) shows the current efficiency and power efficiency as a function of current density for Alq<sub>3</sub> to Alq<sub>3</sub>:T5 devices, respectively. It is clearly observed in figure 5 (a) and (b) that the trend in efficiencies is consistent with the variation of electrical properties of devices with the use of different ETLs and the improved electrical properties lead to the enhanced device efficiency. These results indicate that the TiOPc doping provides a balance of carrier. The control of both carriers in the device gives high yield electroluminescence. At 35.19 mA/cm<sup>2</sup> current density, the current efficiency of Alq<sub>3</sub>: T2 is five times comparing to Alq<sub>3</sub> devices. At current density of 10 mA/cm<sup>2</sup>, the power efficiency of Alq<sub>3</sub>: T2 device increased two times compare to pristine Alq<sub>3</sub> device. The overall current efficiency and power efficiency has increased for 2% doped devices.

The capacitance - voltage (C-V) studies provides electronic properties of OLEDs. The C-V characteristics were measured at a fixed frequency of 1000 Hz under the dark condition as shown in Figure 6. At negative to positive bias (-4 to 4 V); constant capacitance was observed that corresponds to the geometrical capacitance of the device. The capacitance of all devices starts increasing with increase of bias voltage (above 4 V) and after reaching maximum values, they start to decrease for further increase of bias voltage. The increase of capacitance may be due to the accumulation of charges at the Alq<sub>3</sub>: TiOPc interface. As the electrons and holes recombined, the charge is annihilated, thus the capacitance decreases rapidly with the increasing of applied bias. Since,  $V_t \neq V_{bi}$  it simply means that a negative interfacial charge density  $\sigma_{if}$  is present. Its value can be calculated from the following equation:[33,34]

$$\sigma_{if} = Q_{if}/A = \frac{\epsilon_0 \epsilon_r}{d_{Alq_3:T}} \cdot (V_t - V_{bi}) \quad \text{-----} \quad (3)$$

With  $\epsilon_r \approx 3$ ,  $A = 6 \text{ mm}^2$  and  $d_{\text{Alq}_3} = 30 \text{ nm}$ , The  $Q_{\text{if}}$  and  $\sigma_{fi}$  for all studied devices  $\text{Alq}_3$  to  $\text{Alq}_3:\text{T5}$  are  $-2.95, -2.9, -4.6, -4.2, -2.5 \text{ nC}$  and  $-0.49, -0.48, -0.77, -0.7, -0.42 \text{ mC/m}^2$ , respectively. In case of no interfacial charge the threshold voltage and the built-in voltage would be equal ( $V_t = V_{bi}$ ), as the flat-band case would be reached simultaneously in the TiOPc and the  $\text{Alq}_3$  layer.

The Cole-Cole plots of all devices at 0 V bias and room temperature are shown in figure 7. The equivalent circuit of these devices consists of a parallel resistance ( $R_P$ ) and capacitance ( $C_P$ ) network in series with the contact resistance ( $R_S$ ). The  $R_S$  circuit element that corresponds to the intersection of the semicircle at high frequencies represents resistive losses at ITO and Al electrodes. In this work, we have shown the equivalent  $R$ - $C$  electrical circuit for a three layered structure of a device, NPB is the hole transporting layer,  $\text{CBP}:\text{Ir}(\text{ppy})_3$  is the emissive layer and  $\text{Alq}_3:\text{T}$  is the electron Transport layer, which consists of three parallel  $R$ - $C$  circuits connected in series with contact resistance ( $R_S \sim 0\Omega$ ) as inset of figure 7. From figure 7, it is observed that the diameter of the semicircle is highly dependent on the resistance of the devices, which represents the bulk resistance of organic layers  $R_{b1}$  to  $R_{b3}$ . The decrease in the diameter of the semicircle is in response to the increase of the resistance of TiOPc doped  $\text{Alq}_3$  layer which is also reflected in J-V characteristics (figure 4). The equivalent resistance for devices  $\text{Alq}_3$  to  $\text{Alq}_3:\text{T5}$  are  $10\text{M}\Omega$ ,  $8\text{M}\Omega$ ,  $70\text{k}\Omega$ ,  $90\text{k}\Omega$  and  $6\text{M}\Omega$ , respectively.

## Conclusion

In conclusion, the doping of TiOPc in  $\text{Alq}_3$  contributes for increase of electron mobility in  $\text{Alq}_3$  as a result the performance of related OLED enhance. The increase in

mobility is attributed to the addition of new hopping sites for carriers after doping. The surface roughness increases with doping concentrations, the optimized roughness is found to be 0.5742nm for 2% doping. The electron transport is well described by space-charge limited current in the doped and pristine studied thin films of Alq<sub>3</sub>. The electron mobility of 2% doped thin films is  $0.17 \times 10^{-5} \text{ cm}^2 \text{ V}^{-1} \text{ s}^{-1}$  which is three order increases compare to Alq<sub>3</sub> film. The electro-luminescence ( $\sim 7800 \text{ cd/m}^2$ ) at a current density  $10 \text{ mA/cm}^2$  is 2.6 times higher than the undoped device. The interfacial charge density for 2% doped OLEDs device is  $-0.77 \text{ mC/m}^2$ . The Cole-Cole plot of the OLEDs can be modeled as the combination of three parallel resistance-capacitance (*R-C*) equivalent circuits with a series resistance ( $R_S \sim 0 \Omega$ ) of the devices. The equivalent resistance of the optimized device (2% doped) is  $70 \text{ k}\Omega$  where as other devices resistances are in Mega-ohm range.

### Acknowledgements

The authors gratefully recognize the financial support from the Council of Scientific and Industrial Research (CSIR), India for funding our research work.

### References:

- [1] C.W. Tang, V. Slyke, Appl. Phys. Lett. 51 (1987) 913.
- [2] C.W. Tang, V. Slyke, C.H. Chen, J. Appl. Phys. 65 (1989) 3610.
- [3] M.A. Baldo, D.F. O'Brien, Y. You, et al. Nature (London), 395 (1998) 151.
- [4] V.E. Choong, S. Shi, J. Curless, et al. Appl. Phys. Lett. 75 (1999) 172.
- [5] S.A.V. Slyke, C.H. Chen, C.W. Tang, Appl. Phys. Lett. 69 (1996) 2160.
- [6] R. Steyrlleuthner, S. Bange, D. Nehar, J. Appl. Phys. 105 (2009) 064509.
- [7] L.S. Hung, C.W. Tang, M.G. Mason, Appl. Phys. Lett. 70 (1997) 152.

- [8] Z. Xu, L.M. Chen, G. Yang, C.H. Huang, J. Hou, Y. Wu, G. Li, C.S. Hsu, Y. Yang, *Adv. Funct. Mater.* 19 (2009) 1227.
- [9] M. Pope, C.E. Swenberg, *Electronic Process in Organic Crystals and Polymers* (Oxford University Press, Oxford, U.K, 1999).
- [10] M. Pfeiffer, A. Beyer, T. Fritz, K. Leo, *Appl. Phys. Lett.* 73 (1998) 729.
- [11] M. Pfeiffer, A. Beyer, T. Fritz, K. Leo, *Appl. Phys. Lett.* 73 (1998) 3202.
- [12] M. Pfeiffer, T. Fritz, J. Blochwitz, A. Nollau, B. Plonnigs, A. Beyer, K. Leo, *Adv. Solid State Phys.* 39 (1999) 77.
- [13] C. Ganzorig, M. Fujihira, *Appl. Phys. Lett.* 77 (2000) 4211.
- [14] X. Zhou, M. Pfeiffer, J. Blochwitz, A. Werner, A. Nollau, T. Fritz, K. Leo, *Appl. Phys. Lett.* 78 (2001) 410.
- [15] A. Kumar, R. Srivastava, P. Tyagi, D.S. Mehta, *J. Appl. Lett.* 109 (2011) 114511.
- [16] K. R. Choudhury, J.H. Yoon, F. So, *Adv. Mater.* 20 (2008) 1456.
- [17] Y. Shirota, H. Kageyama, *Chem. Rev.* 107 (2007) 953.
- [18] V. Coropceanu, J. Comil, D.A.S. Filho, Y. Oliver, Y. Silve, J.L. Bredas, *Chem. Rev.* 107 (2007) 926.
- [19] W. Brutting, S. Berleb, A.G. Muckl, *Org. Electron.* 2 (2001) 1.
- [20] K. Walzer, B. Maening, M. M. Pfeiffer, K. Leo, *Chem. Rev.* 107 (2007) 1233.
- [21] W. Ou-yang, M. Weis, X. Chen, T. Manaka, M. Iwamoto, *J. Chem. Phys.* 131 (2009) 104702.
- [22] Y. Zhou, C. Fuentes-Hernandez, J. Shim, J. Meyer, A.J. Giodano, H. Li, P. Winget, T. Papadopoulos, H. Cheun, J. Kim, M. Fenoll, A. Dindar, W. Haske, E. Najafabadi, T.M. Khan, H. Sojoudi, S. Barlow, S. Graham, J.L. Bredas, S.R. Marder, A. Khan, B. Kippelen, *Science* 336 (2012) 327.

- [23] D. Taguchi, T. Shino, X. Chen, L. Zhang, J. Li, M. Weis, T. Manaka, M. iwamoto, J. Appl. Phys. 110 (2011)103717.
- [24] Y.H. Deng, Y.Q. Li, Q.D. Ou, Q. K. Wang, F.Z. Sun, X.Y. Chen, J.X. Tang, Org. Electron. 15 (2014) 1215.
- [25] J. Kido, K. Nagai, Y. Okamoto, IEEE. 40 (1993) 1342.
- [26]. J. Kido, T. Matsumoto, Appl. Phys. Lett. 73 (1998) 2866.
- [27] A. Werner, F. Li, K. Harada, M. Pfeiffer, T. Fritz, K. Leo, S. Machill, Adv. Func. Mater. 14 (2004) 255.
- [28] R.Q. Zhang, C.S. Lee, S.T. Lee, J. Chem. Phys. 112 (2000), 8614.
- [29] H. Ishii, K. Sugiyama, E. Ito, K. Seki, Adv. Mater. 11 (1999), 605.
- [30] G.G. Malliaras, Y. Sen, D.H. Dunlup, H. Murata, Z.H. Kafafi, Appl. Phys. Lett. 79 (2001) 2582.
- [31] O. Tal, Y. Rosenwaks, Y. Preezant, N. Tessler, C. K. Chan, and A. Kahn, PRL **95**, (2005) 256405
- [32] Po-Ching Kao, Jie-Han Lin, Jing-Yuan Wang, Cheng-Hsien Yang, Sy-Hann Chen, JOURNAL OF APPLIED PHYSICS 109, (2011) 094505
- [33] W. Brutting, S. Berleb, A. G. Muckl, Org. Electron. 2 (2001) 1.
- [34] S. Nowy, W. Ren, J. Wagner, J.A. Weber, W. Brutting, Proc. of SPIE Vol. 7415 (2009) 74150G-1.

**Figure captions**

**Figure 1** The AFM images ( $5\ \mu\text{m} \times 5\ \mu\text{m}$ ) TiOPc doped Alq<sub>3</sub> thin film (A) Alq<sub>3</sub>, (B) Alq<sub>3</sub>:T1, (C) Alq<sub>3</sub>: T2, (D) Alq<sub>3</sub>:T3 and (E) Alq<sub>3</sub>:T5.

**Figure 2** The Current density - Voltage (*J-V*) characteristics of the electron only devices of Alq<sub>3</sub>:TiOPc thin film. The structure of device Al/Alq<sub>3</sub>: T (1-5%)/Al. Inset- the enlarged *J-V* characteristics with log of x axis.

**Figure 3** (A) The molecular structure of TiOPc and Energy level diagram of OLEDs (B) The electroluminescence spectra of the OLED at different bias voltage; inset- the camera image of light output at 8V and 15V bias voltage

**Figure 4** The Current density-Voltage-Luminescence (*J-V-L*) characteristics of devices for different doping of TiOPc with Alq<sub>3</sub>

**Figure 5 (a)** Current efficiency Vs current density characteristics of the Alq<sub>3</sub>, Alq<sub>3</sub>:T(1, 2,3 &5%) devices (b) Power efficiency-current density characteristics of the Alq<sub>3</sub>, Alq<sub>3</sub>:T(1, 2,3 &5%) devices.

**Figure 6** Capacitance-Voltage (*C-V*) characteristics of OLED at a frequency of 1000 Hz.

**Figure 7** Cole-Cole plot of Alq<sub>3</sub>, Alq<sub>3</sub>:T(1, 2,3 &5%) OLEDs at 0 V bias, Inset - the enlarged curve of Alq<sub>3</sub>:T2 and Alq<sub>3</sub>:T3 devices.

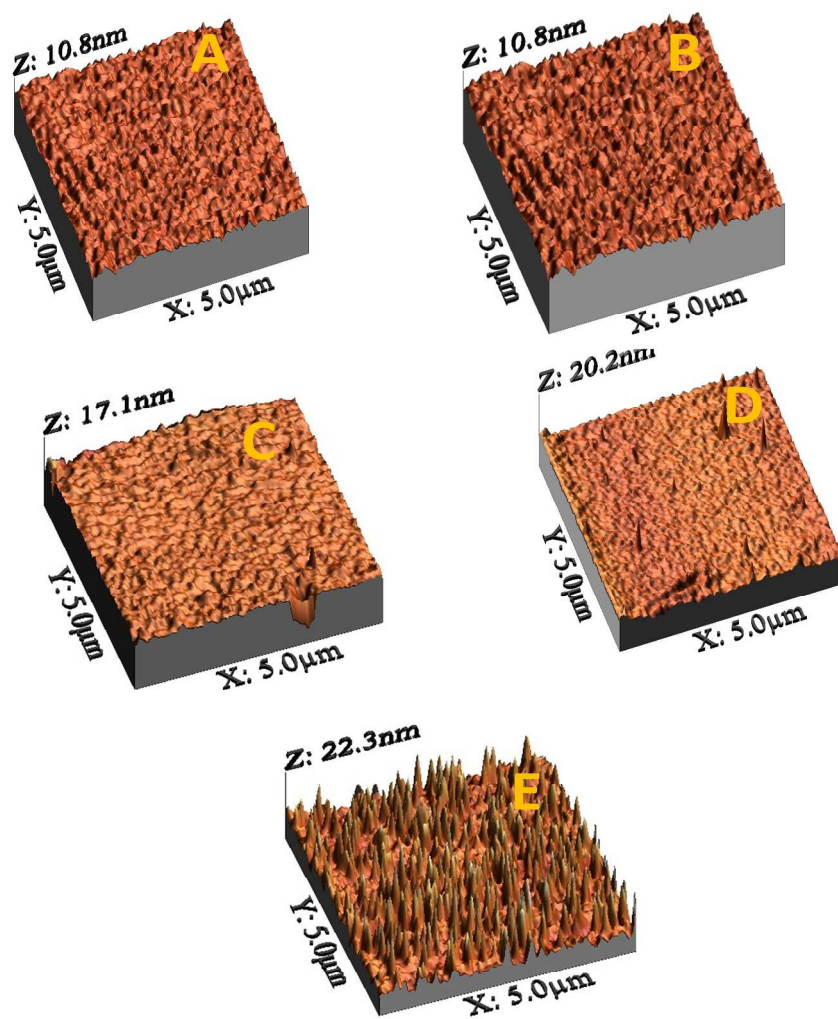


Figure 1

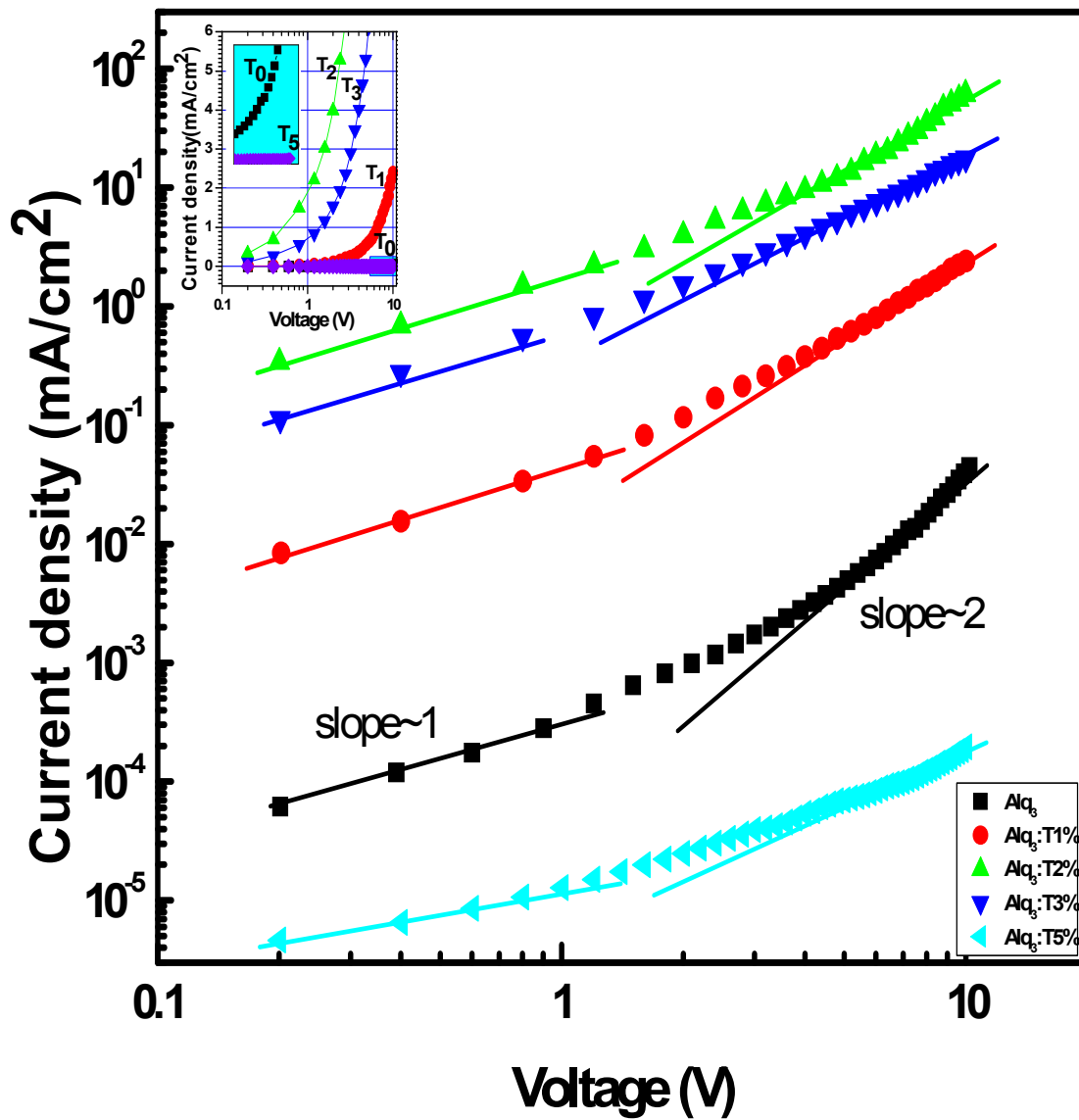


Figure 2

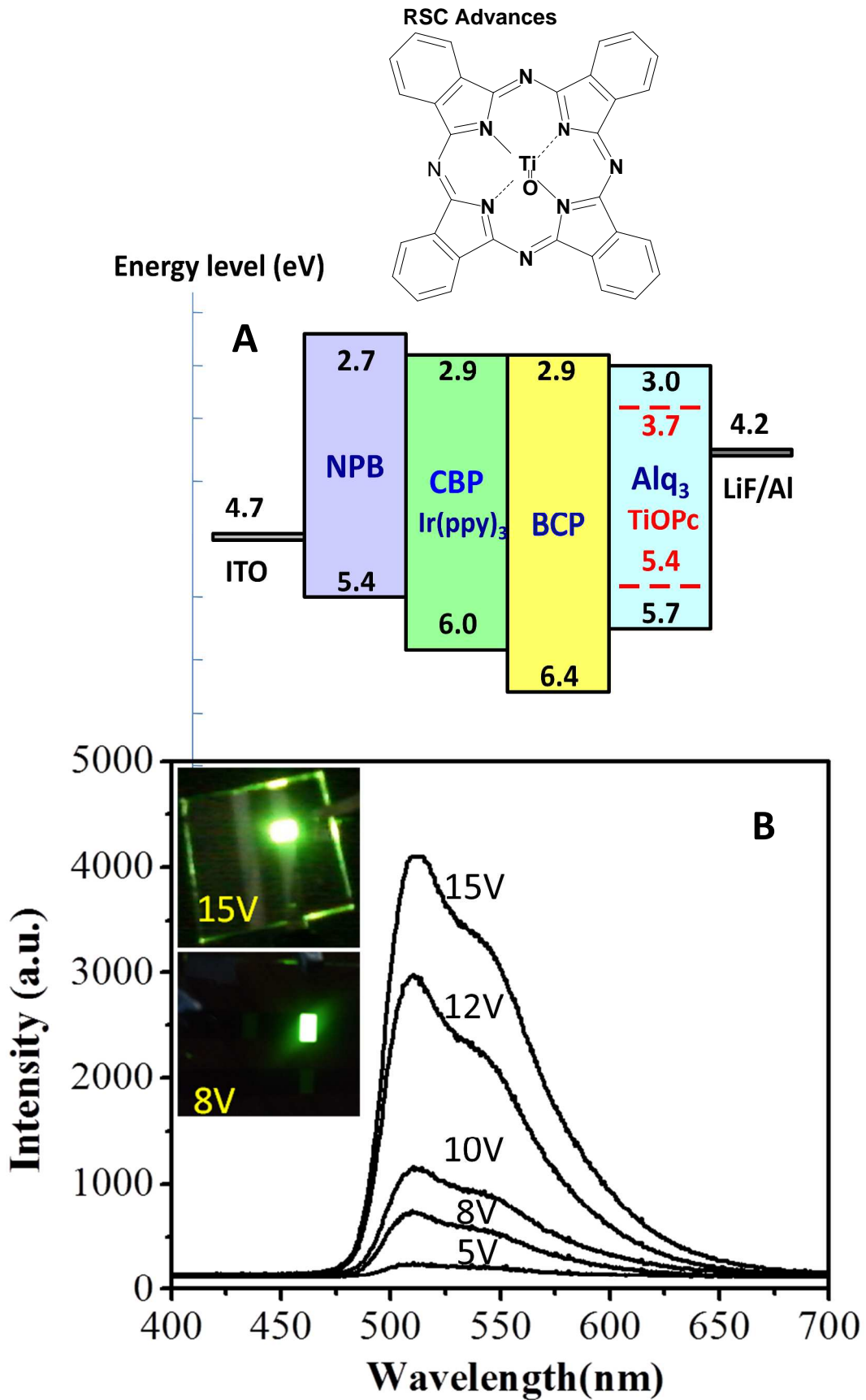


Figure 3

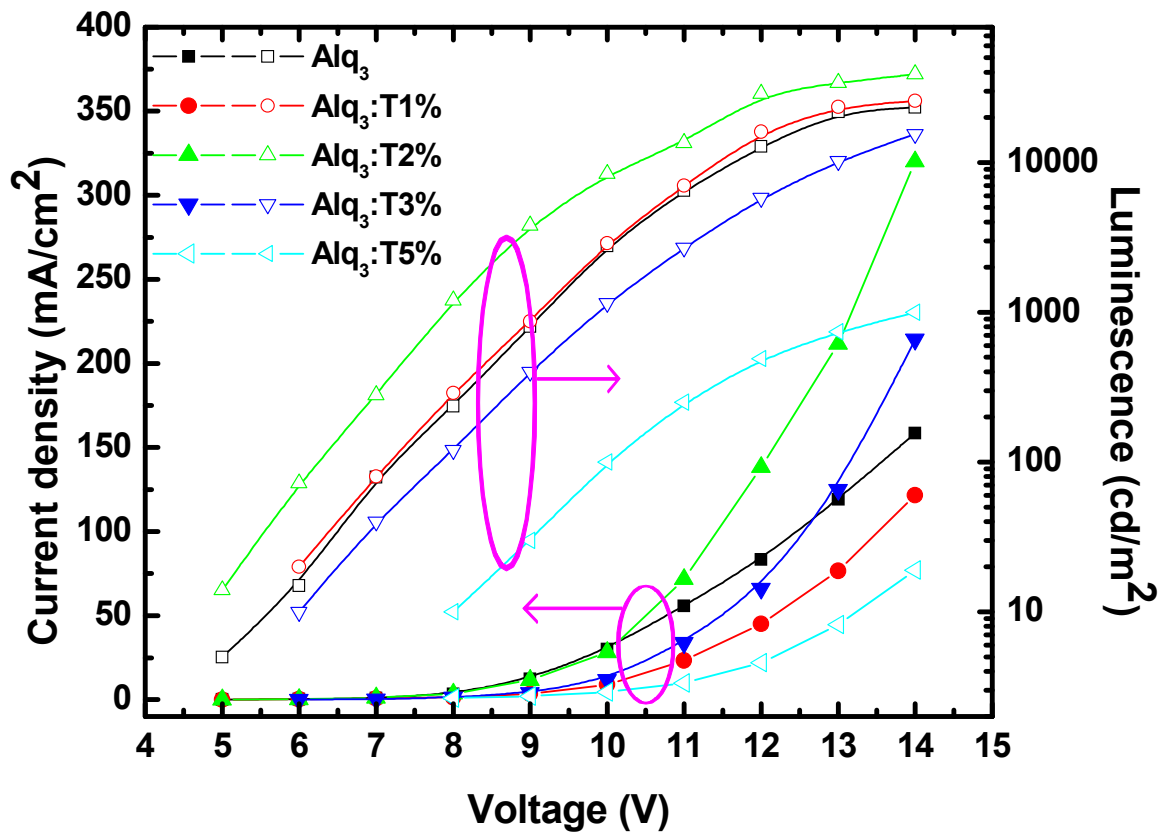


Figure 4

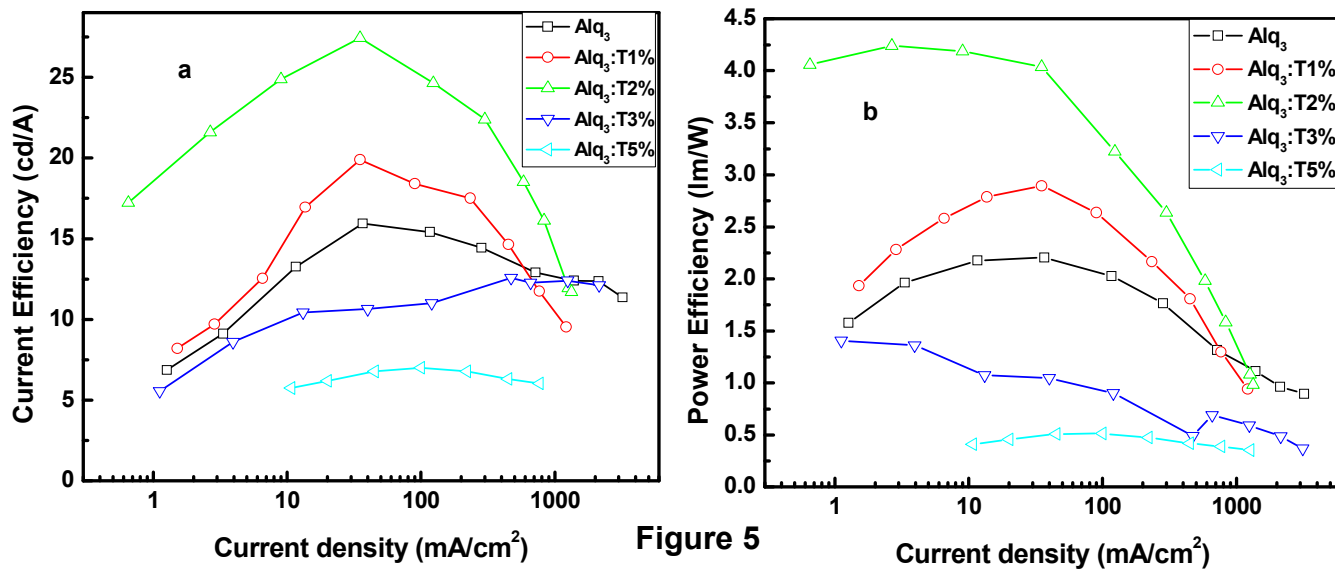


Figure 5

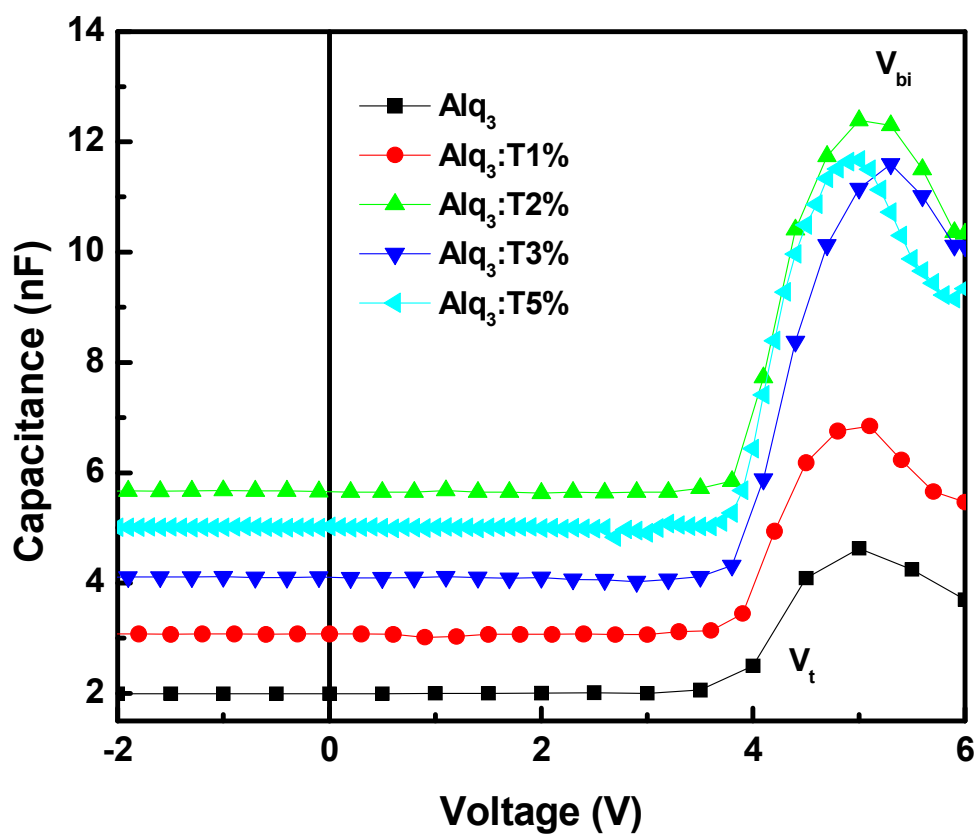


Figure 6

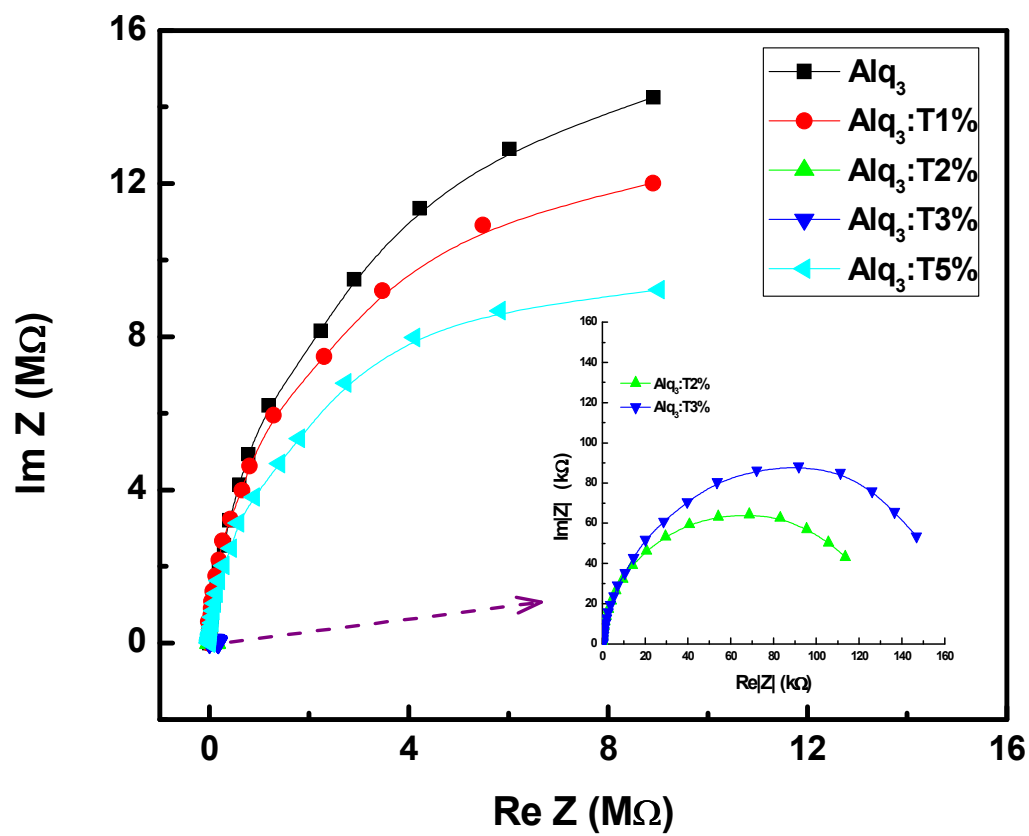


Figure 7